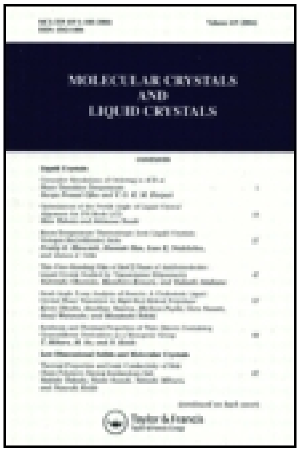

Molecular Crystals and Liquid Crystals Science and Technology. Section A. Molecular Crystals and Liquid Crystals
Publication details, including instructions for authors and subscription information:
http://www.tandfonline.com/loi/gmcl19

Birefringence and Refractive Indices Dispersion of Different Liquid Crystalline Structures

Jorg Schirmer [a] , Peter Kohns [a] , Theodor Schmidt-kaler [a] , Anatoli A. Muravski [b] , Sergei Ye. Yakovenko [b] , Vladimir S. Bezborodov [b] , Roman Dabrowski [c] & Povilas Adomenas [d]
[a] Optikzentrum NRW, Universitätsstraße 142, D-44799, Bochum, Germany
[b] Institute of Applied Physics Problems, Kurchatova 7, Minsk, 220064, Rep. Belarus
[c] Military University of Technology, Institute of Chemistry, 01-489, Warsaw 49, Poland
[d] University of Vilnius, Liquid Crystals Lab., 2734, Vilnius, Universiteto St. 3, Lithuania

Version of record first published: 04 Oct 2006

To cite this article: Jorg Schirmer, Peter Kohns, Theodor Schmidt-kaler, Anatoli A. Muravski, Sergei Ye. Yakovenko, Vladimir S. Bezborodov, Roman Dabrowski & Povilas Adomenas (1997): Birefringence and Refractive Indices Dispersion of Different Liquid Crystalline Structures, Molecular Crystals and Liquid Crystals Science and Technology. Section A. Molecular Crystals and Liquid Crystals, 307:1, 17-42

To link to this article: http://dx.doi.org/10.1080/10587259708047084

Mol. Cryst. Liq. Cryst., 1997, Vol. 307, pp. 17–42
Reprints available directly from the publisher
Photocopying permitted by license only

Birefringence and Refractive Indices Dispersion of Different Liquid Crystalline Structures

JORG SCHIRMER[a], PETER KOHNS[a],
THEODOR SCHMIDT-KALER[a], ANATOLI A. MURAVSKI[b],
SERGEI YE. YAKOVENKO[b], VLADIMIR S. BEZBORODOV[b],
ROMAN DABROWSKI[c] and POVILAS ADOMENAS[d]

[a]*Optikzentrum NRW, Universitätsstraße 142, D-44799 Bochum, Germany;*
[b]*Institute of Applied Physics Problems, Kurchatova 7, Minsk, 220064, Rep. Belarus;*
[c]*Military University of Technology, Institute of Chemistry, 01-489 Warsaw 49, Poland;*
[d]*University of Vilnius, Liquid Crystals Lab., 2734 Vilnius, Universiteto St. 3, Lithuania*

(Received 3 July 1996; In final form 17 February 1997)

The birefringence and refractive indices of several liquid crystalline structures were measured throughout the visible wavelength region (400–900 nm) at different temperatures. Mixtures composed of members of the same homologous series were used in order to achieve the nematic phase at room temperature. Data on 28 mixtures, mainly with cyclohexane – phenyl and biphenyl cores, are presented. The set includes widely used structures as well as newly synthesized. Some details of experimental methods, formulas for interpolation of the results and observed regularities are briefly discussed.

Keywords: Liquid crystals; birefringence; refractive index; dispersion; chemical structure

INTRODUCTION

Most technical applications of liquid crystals (LC) are based on their specific optical properties, but LC producers usually present in their catalogues the birefringence and refractive indices of their mixtures only at one wavelength. Thus, optical parameters of LC devices to be constructed are estimated based on this value and at the early stages of the development this was sufficient. Nowadays, the main trends in the market of LC devices are to improve the parameters of the existing devices and to find new areas for application of LC materials.

To improve optical operation means to optimize such optical properties as luminance, contrast and gray levels in the whole visible spectrum. Much effort is done in this field: LC displays are made more achromatic [1, 2], with improved viewing angle [3, 4], with higher contrast [4, 5]. LC devices are used in such new areas as phase retarders, correctors etc. [6] not only in the visible, but also in the near infrared.

All these aspects require the knowledge of the refractometric data of LC in the whole spectrum of operation. In many cases optical properties of a device depend on the product of birefringence and the LC layer thickness. The wavelength dependence of the optical properties, for example phase retardation, is determined by the product of birefringence dispersion and thickness. Thus by choosing appropriate combinations of LC thickness, birefringence and birefringence dispersion the optical properties of a device can be varied to some extent independently at different wavelengths. For this the dispersion characteristics of LC's in the wavelength region of interest must be known.

With this work we provide such information. Using refractometric and interferometric methods we determined the birefringence and the refractive indices of different classes of liquid crystalline materials widely used in commercial mixtures. We tried to cover as many different classes of LC materials as were available to us. Although the set which we present in this paper in no case can be treated as complete we hope that it can help the designers to develop mixtures appropriate for their devices, or at least to find guidelines for their development.

We studied not individual compounds, but mixtures, containing compounds of some homologous series. The main goal which we pursued taking mixtures was to obtain mesophase at room temperature (when it was possible) and thus to make these substances more attractive to designers.

A discussion of advantages and disadvantages of various methods for refractive indices determination is beyond the scope of this work, so in the experimental section we only describe the methods we used for this and give overall precisions for the data. In the third section the composition of LC's and the data are presented with explanations of the tables contents and brief comments on the observed properties.

EXPERIMENTAL

The method used for birefringence dispersion measurements was proposed by Wu *et al.* [7]. A filled liquid crystal cell with planar alignment is placed between two polarizers in such a way, that the director of the liquid crystal is oriented at an angle of $\alpha = 45^\circ$ with respect to the transmission direction of the first polarizer. The birefringent LC introduces a phase retardation δ between extraordinary and ordinary wave which is analyzed by the second polarizer, oriented at an angle β with respect to the first polarizer. If the LC layer is sufficiently thin, absorption anisotropies between extraordinary and ordinary wave can be neglected. Denoting with T the transmission of the LC cell without polarizers including reflection losses at the glass surfaces and absorption losses, the transmissions $T_\perp$ and $T_\parallel$ for perpendicular ($\beta = 90^\circ$) and parallel ($\beta = 0^\circ$) oriented polarizers are [7]:

$$T_\perp = T\sin^2(\delta/2) = \tfrac{1}{2}T[1 - \cos\delta]$$

$$T_\parallel = T\cos^2(\delta/2) = \tfrac{1}{2}T[1 + \cos\delta] \qquad (1)$$

From these measured light transmissions the phase retardation δ and subsequently the birefringence Δn of the LC under study can be evaluated, provided that the thickness d_{LC} of the LC layer is known:

$$\delta = 2\pi\mathrm{INT}(\tfrac{N}{2}) - (-1)^N 2\tan^{-1}\left[\left(\frac{T_\perp}{T_\parallel}\right)^{1/2}\right]; \quad N = 1, 2, \ldots \qquad (2)$$

$$\Delta n = \frac{\delta\lambda}{2\pi d_{\mathrm{LC}}} \qquad (3)$$

In Equation 2 INT($N/2$) refers to the integer function.

In order to determine continuous birefringence values over the entire visible spectrum a tungsten lamp was taken as the lightsource and a diode line spectrometer served as the detector. With this combination a signal to noise ratio better than 1% in the wavelength range 400 to 900 nm was achieved. The spectral resolution due to the spectrometer slit width was 10 nm, the pixel size corresponds to 3.3 nm and the accuracy of wavelength calibration was 0.3 nm. The polarizers used were Glan type polarizing prisms made of calcite with an extinction ratio better than 10^{-5} within the wavelength region of interest. The LC's under study were filled into commercially available indium-tin-oxide (ITO) coated testcells with polyimide alignment layers. Mean thicknesses of ITO and polyimide were 35 nm and 30 nm according to the producers information. Cells with ~ 4 µm and ~ 10 µm LC thickness were used. The thickness was determined interferometrically before filling the cell by determination of the angles of destructive interference in reflection geometry [8] with a helium neon laser as light source. Temperature stabilization within ± 0.02 K was achieved using a thermocell equiped with Peltier thermoelement, temperature sensor and regulation circuit.

Figure 1 gives an example of raw experimental data. In addition to the transmissions corresponding to Equation 1 the transmission T_o for the case polarizer and analyzer parallel ($\beta = 0°$) and LC director at angle $\alpha = 90°$, i.e. for the ordinary wave, is shown.

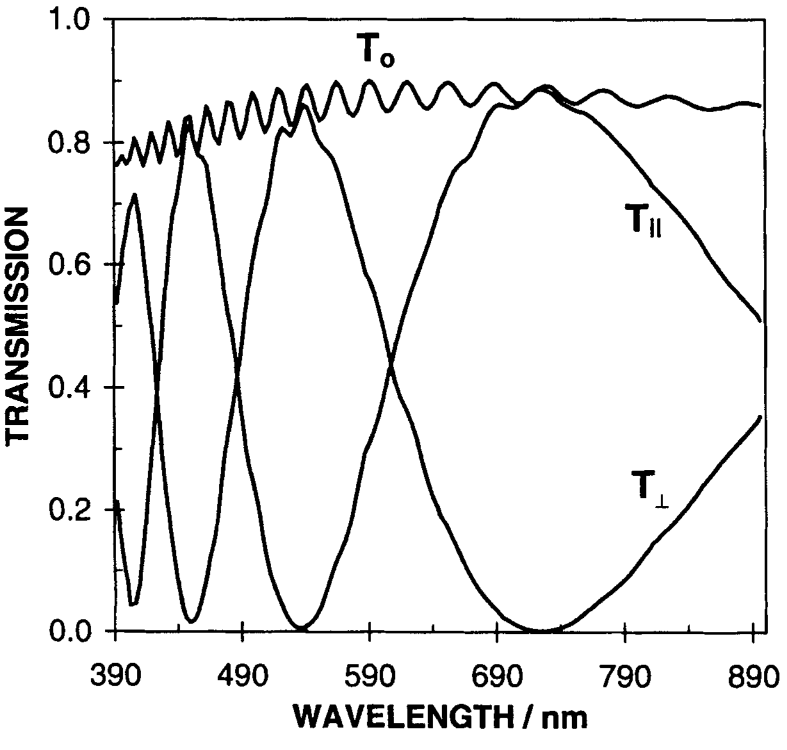

FIGURE 1 Measured transmissions of the polarizer – LC cell – analyzer system for three combinations of angles α between polarizer and LC director and β between polarizer and analyzer. T_o corresponds to the transmission of the ordinary wave ($\alpha = 90°$, $\beta = 0°$). $T_{\perp}$ and $T_{\parallel}$ refer to the conditions ($\alpha = 45°$, $\beta = 90°$) and ($\alpha = 45°$, $\beta = 0°$), respectively. Data are for LC mixture number 7 (see Tab. I).

Three features are obvious:

1. Reflection and absorption losses degrade the transmission of the cell to less than 90%.
2. Especially in the short wavelength region the ratio $T_\perp / T_\parallel$ does not approach zero or infinity at wavelengths corresponding to multiples of halfwave phase retardation ($\delta = N\pi$) as it is expected from Equation 1.
3. All transmissions show periodic modifications on a percent scale due to interferences within the LC cell.

These features affect the calculation of birefringence dispersion curves if Equations 1 to 3 are used without the corrections described in the following.

First the transmission T of the LC cell (see Equation 1) is determined from the maxima in the measured transmission T_o of the ordinary wave. For wavelength between these a linear interpolation is used.

Feature 2 arises from integrations over wavelength (spectral resolution of the spectrometer) and cell thickness (quality of inner cell surfaces), both together yielding an integration over a phase retardation interval $[\delta - \Delta\delta, \delta + \Delta\delta]$, as well as from depolarization of the ordinary and the extraordinary wave due to director fluctuations of the LC. The effect on the birefringence dispersion curve as calculated from Equations 2 and 3 are steps in birefringence values at the wavelengths corresponding to $\delta = N\pi$ where the function $(-1)^N \tan^{-1}$ changes its sign. Performing the integration on Equation 1 we obtain:

$$
\begin{aligned}
T_{\substack{\perp\\ \parallel}}(\delta) &= \frac{1}{2\Delta\delta}\frac{1}{2}T\int_{\delta-\Delta\delta}^{\delta+\Delta\delta}[1 \mp \cos\delta]\,d\delta \\
&= \frac{1}{2}T\left[1 \mp \left(\frac{\sin\Delta\delta}{\Delta\delta}\right)\cos\delta\right] \\
&= \frac{1}{2}T\left[1 \mp \left(1 - \frac{(\Delta\delta)^2}{3!} + \frac{(\Delta\delta)^4}{5!} \mp \ldots\right)\cos\delta\right] \qquad (4)
\end{aligned}
$$

From solving Equation 3 for δ and using the extreme values of the wavelength to thickness fraction $(d_{\mathrm{LC}} \pm \Delta d)/(\lambda \mp \Delta\lambda)$ it is seen that $\Delta\delta$ incorporates wavelength dependences proportional to λ^{-1} and λ^{-2}. Therefore correction terms proportional to λ^{-n} with $n \geqslant 2$ should be accounted for in Equation 4. In addition the depolarization due to director fluctuations is known [9] to be proportional to λ^{-4}. The experience from our measurements showed that within the experimental scattering it is sufficient to account only for this wavelength dependence. Thus instead of Equation 1 we use Equation 5 for data reduction:

$$T_{\perp}(\delta)=\frac{1}{2}T(\delta)\left[1 \mp (1-A\cdot\lambda^{-4})\cos\delta\right] \qquad (5)$$

The coefficient A is determined at the wavelengths where the transmissions $T_{\perp}$ and T have their minima and is interpolated linearly between these wavelengths. The magnitude of the correction $A\cdot\lambda^{-4}$ is usually well below 0.1 and depends on cell quality and birefringence.

The interferences within the LC cell (feature 3) are caused mainly by reflections at the high refractive index ITO coatings resulting in a transmission similar to an etalon with different optical thicknesses for the ordinary and the extraordinary wave. This effect yields a sinusoidal modulation of the resulting birefringence dispersion curve with an amplitude of a few percent and a modulation length equal to the interference cycles of the ordinary wave. The correction for this effect is described elsewhere [10]. It can be shown that a simple smoothing of the birefringence dispersion curve calculated without this correction gives correct results.

The results of Δn measurements were confirmed for some liquid crystals by determining the wavelength of extrema (where $\delta = N\pi$) in transmission interference spectra according to Equations 1 to 3. For these independent measurements thicker cells (20 μm) and a spectrometer with higher spectral resolution (type SPECORD-M40) were used. From repeated measurements of the same liquid crystals in different cells, with various spectrometer modules and experimental setups over a period of one year the reproducibility of Δn values is ± 0.001 within the spectral range 400 nm to 900 nm.

It is possible to determine ordinary refractive indices for a number of wavelengths from the positions λ_k of interference maxima and minima in the transmission T_o of the ordinary polarized light. The wavelengths λ_k are determined with sub pixel accuracy using quadratic interpolations. The phase shift of the first order reflections with respect to the directly transmitted beam equals a multiple of one wavelength phase retardation for transmission maxima. If we neglect the influence of the ITO and polyimide films we can calculate n_o according to the formula (for minima the integer value k is replaced by $k + 1/2$):

$$n_o(\lambda_k)=\frac{k\lambda_k}{2d_{\mathrm{LC}}} \qquad (6)$$

The interference order k is found by solving Equation 6 for two subsequent maxima with the assumption $n_o(\lambda_{k+1}) = n_o(\lambda_k)$. The evaluation of the phase shift caused by the ITO and polyimide films (see appendix) reveals that Equation 6 has to be modified. With φ_r denoting the phase change on reflection at one ITO film and $\delta_p = 2\pi n_p d_p/\lambda$ the phase retardation due to one polyimide film we find for interference maxima:

$$n_o(\lambda_k) = \left(k + \frac{\varphi_r - 2\delta_p}{\pi}\right)\left(\frac{\lambda_k}{2d_{\mathrm{LC}}}\right) \tag{7}$$

Equation 7 is used for the calculation of the ordinary refractive indices. Since interferences are less pronounced for the extraordinary wave we calculate extraordinary refractive indices from n_o and Δn. From the discussion in the appendix we estimate the precision of refractive indices to be ± 0.005 within the wavelength region 400 nm to 900 nm. Wavelength independent errors due to the uncertainty in cell thickness determination are corrected for by calibrating the determined birefringence and refractive indices with refractometer measurements at 589 nm.

Figure 2 shows the birefringence and refractive indices dispersions derived from the raw data of Figure 1 (20°C) and an equivalent measurement at 30°C.

RESULTS

The compositions in weight % and clearing temperatures of the LC mixtures investigated are given in Table I. All the compounds were prepared by ourselves. The compounds 17, 18 and 19 are new ones. The synthesis of 18 is described in Ref. [11] and the synthesis of 17 and 19 in Ref. [12]. The other liquid crystals are well known in literature and references for them are listed in [13].

In order to give analytical expressions for the wavelength dependence of birefringence and refractive indices we used the single band model [14] to fit the experimental data. This model incorporates one averaged resonance wavelength in the ultraviolet wavelength range and a parameter $G(T)$ describing besides molecular parameters mainly the temperature dependence of the order parameter of the liquid crystal. Equation 8a is for birefringence, Equation 8b for ordinary and extraordinary refractive indices:

$$\Delta n(\lambda, T) = G(T)\frac{\lambda^2 \lambda_0^2}{\lambda^2 - \lambda_0^2} \tag{8a}$$

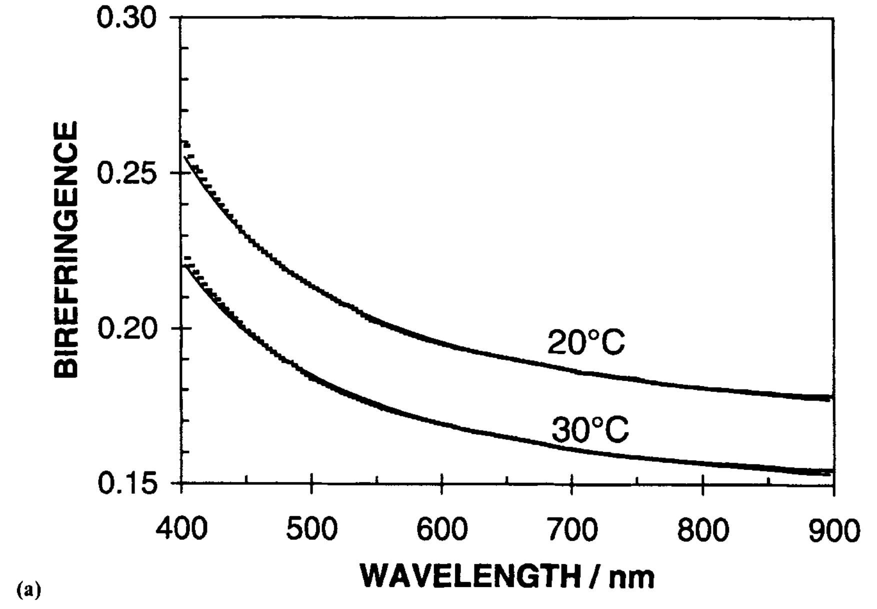

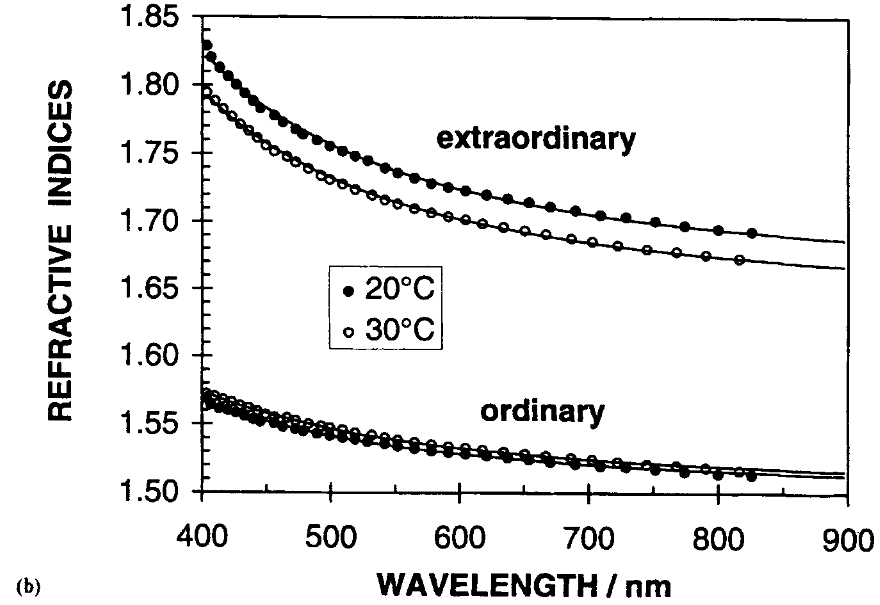

FIGURE 2 Birefringence and refractive indices dispersion of mixture number 7 (PP), calculated from the data of Figure 1. Thin straight lines represent the two parameter fits according to Equation 8.

TABLE I Composition of LC mixtures. The abbreviations follow the analogous system for liquid crystal compounds which was proposed by Hoffmann La Roche's Laboratory. Alkyl chains with *n* carbon atoms (C_nH_{2n+1}) are named R_n with *n* given in the third column

NO	COMPOSITION	n	m	wt%	T_{NI}/°C
1	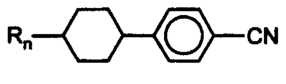 nCP	3 5 7		29.67 33.33 37.00	53.0
2	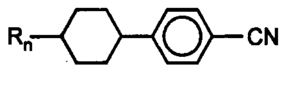 nCP	2 4 6		29.46 33.34 37.20	34.5
3	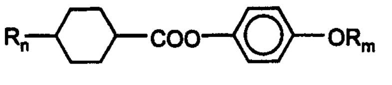 nCEPOm	4 4 4	1 2 5	30.95 32.44 36.61	65
4	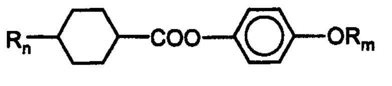 nCEPOm	5 5 5	1 2 3	32.83 31.32 35.85	71.5
5	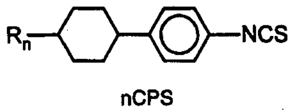 nCPS	3 5 7		64.81 9.26 25.93	42.5- 43.0
6	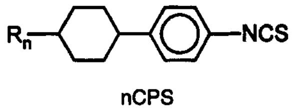 nCPS	4 6 8		30.23 33.34 36.43	40.0
7	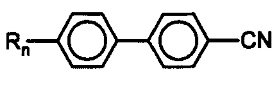 nPP	3 5 7		17.36 39.12 43.52	34.5
8	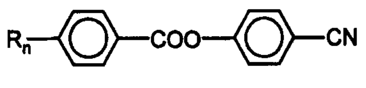 nPEP	4 6 8		30.29 33.33 36.38	46.5

TABLE I (Continued)

9	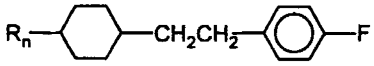 nCAPF	5		50.06	49.5- 54.5
	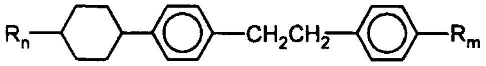 nCPAPm	2 5	3 3	23.52 26.42	
10	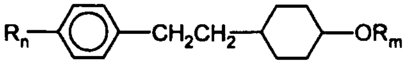 nPACOm	3 5	1 2	51.25 48.75	48
11	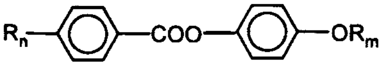 nPEPOm	4	6	51.91	61
	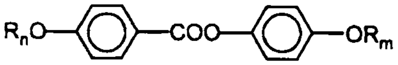 nOPEPOm	1	6	48.09	
12	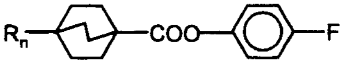 nBEPF	4 7		46.77 53.23	36.5
13	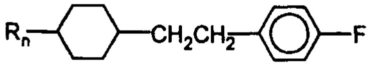 nCAPF	5		65	37- 49
	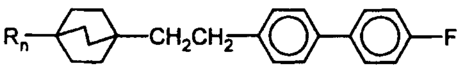 nBAPPF	3 5 6		5 15 15	

TABLE I (Continued)

14	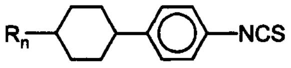 nCPS	2 4 6		23.01 15.71 45.64	59-67
	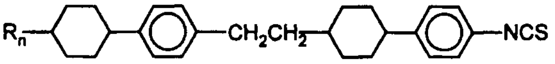 nCPACPS	2 4		3.64 12.00	
15	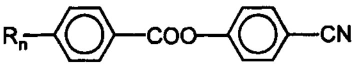 nPEP	4 6 8		19.10 32.49 25.13	85-87
	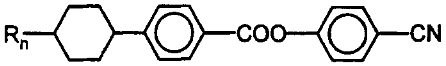 nCPEP	4		23.28	
16	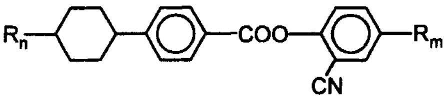 nCPEPm	2 4 4 5 7	5 4 5 4 4	20.0 20.0 20.0 20.0 20.0	104
17	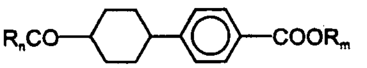 nGCPEm	3 3 3 5 5 5 7 7 7	1 2 3 1 2 3 1 2 9	11.11 11.11 11.12 11.11 11.11 11.11 11.11 11.11 11.11	17.5

TABLE I (Continued)

18	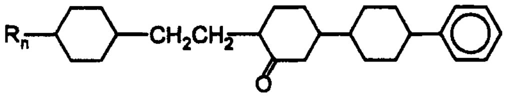 nCANCP	4		7.60	60-66
	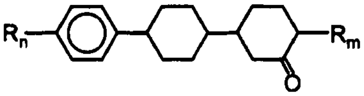 nPCNm	3 3	3 5	3.04 15.19	
	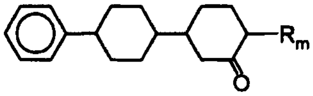 PCNm		5	30.40	
	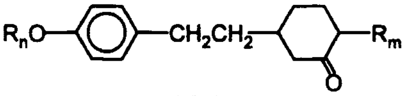 nOPANm	2	5	7.60	
	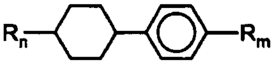 nCPm	3	5	36.17	
19	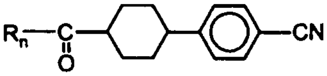 nGCP	3 5 7		20 20 20	43.5-44
	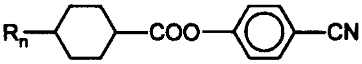 nCEP	3 5		20 20	
20	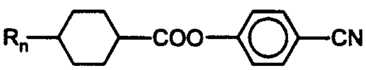 nCEP	3 5		47.5 52.5	74.5

TABLE I (Continued)

21	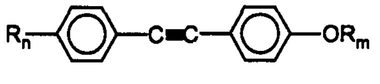 nPZPOm	4	1	25.0	63.0
		4	2	20.0	
		5	1	16.0	
		5	6	16.0	
		8	2	23.0	
22	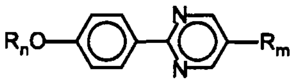 nOPP(1)m	6	8	23.0	S_A
		6	9	20.0	64
		8	7	7.0	N
		8	8	16.0	70
		9	9	16.0	
		10	7	8.0	
		10	8	10.0	
23	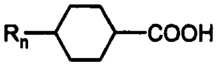 nCE	4		50.0	92
		6		50.0	
24	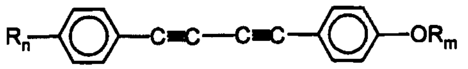 nPZZPOm	2	4	36.0	101
		2	5	31.5	
		4	5	32.5	
25	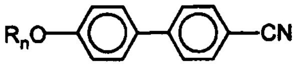 nOPP	3		26.9	70
		5		33.8	
		8		39.3	
26	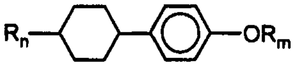 nCPOm	3	2	48.62	31.5
		5	1	51.38	
27	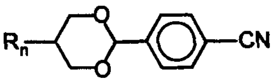 nDP	3		36.95	45.5
		5		33.34	
		7		29.71	

TABLE I (Continued)

28	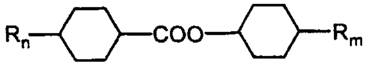 nCECm	3	3	47.73	40.0
		5	3	52.27	

$$n_j(\lambda, T) = 1 + G_j(T)\frac{\lambda^2 \lambda_j^2}{\lambda^2 - \lambda_j^2} \qquad j = o, e \tag{8b}$$

These formulas proved to fit the experimental data within the experimental uncertainty in most cases. Deviations between experimental data and fits slightly higher than the experimental uncertainty occur in the case of the high birefringent LC, as may be seen from the standard deviations given in Table II. This is not surprising because in principle one has to account for several absorption bands in the UV and Equation 8 is valid only far from the lowest frequency one, which in the case of high birefringent LC's is near to the visible wavelength region [14]. A more detailed accounting for the different resonances would require additional measurements of the ultraviolet absorption spectra in order to fix the different resonance wavelengths because otherwise no clear solution for the multiple parameter problem can be found.

Contributions from different absorption bands may change with temperature which consequently leads to changes of λ_0 if Equation 8 is used for fitting. We therefore present the parameters G and λ_0 according to Equation 8 in the Tables II, III and IV for birefringence, ordinary and extraordinary refractive index, respectively, for each temperature measured.

Experimental data were fitted within the wavelength region 400 nm to 900 nm. For refractive indices this interval had to be reduced in some cases either because the spectrometer could not resolve the interferences in the short wavelength region or because the amplitude of the interferences was to low for an accurate determination of maximum and minimum positions in the long wavelength region. However the spectral interval used for fitting is 300 nm or more for all data presented here.

The fourth column in the Tables II, III and IV lists the birefringence and refractive indices determined at 589 nm using an Abbe refractometer. The precision of these values is ± 0.0001 to ± 0.0002, unless otherwise stated.

TABLE II Birefringence of liquid crystal mixtures from refractometric and spectroscopic measurements. Fit parameters λ_0 and G according to Equation 8a and standard deviations σ are for the wavelength range 400 nm to 900 nm

NO	*LC*	$T/^\circ C$	$\Delta n(589\,nm)$	λ_0/nm	$G/10^{-6}\,nm^{-2}$	$\sigma/10^{-3}$
1	nCP	20	0.1213	175.3	3.598	0.36
		30	0.1130	173.2	3.441	0.28
		40	0.1023	176.3	2.996	0.23
		50	0.0786	182.3	2.139	0.21
2	nCP	20	0.1003	184.0	2.673	0.27
		30	0.0760	189.2	1.904	0.18
3	nCEPOm	20	0.0814	164.7	2.767	0.27
		30	0.0776	163.7	2.672	0.16
		40	0.0725	164.6	2.468	0.29
		50	0.0662	156.6	2.510	0.33
4	nCEPOm	20	0.0877	167.4	2.875	0.52
		30	0.0840	167.7	2.744	0.50
		40	0.0797	172.5	2.450	1.03
		50	0.0745	162.1	2.620	1.17
5	nCPS	20	0.1939	220.7	3.421	0.44
		30	0.1783	220.4	3.157	0.46
6	nCPS	20	0.1577	220.6	2.786	0.37
		30	0.1404	219.9	2.499	0.42
7	nPP	20	0.1972	240.5	2.840	0.72
		30	0.1707	239.8	2.476	0.74
8	nPEP	20	0.1659	207.4	3.379	0.45
		30	0.1514	206.6	3.111	0.47
		40	0.1302	206.2	2.687	0.56
9	nCAPF	20	0.0690	145.0	3.083	0.18
	+nCPAPm	30	0.0650	146.3	2.851	0.19
		40	0.0595	143.5	2.718	0.23
10	nPACOm	20	0.0840	155.7	3.222	0.12
		30	0.0793	154.8	3.082	0.09
		40	0.0728	145.9	3.209	0.38
11	nPEPOm	20	0.1403[1]	207.4	2.858	0.30
	+nOPEPOm	30	0.1355[1]	207.3	2.763	0.26
		40	0.1312	207.3	2.675	0.26
		50	0.1189	206.6	2.443	0.28
12	nBEPF	20	0.0569	134.4	2.987	0.28
		30	0.0511	125.4	3.101	0.19
13	nCAPF	20	0.0836	181.3	2.301	0.33
	+nBAPPF	30	0.0786	180.8	2.177	0.21
14	nCPS	30	0.1701	219.4	3.044	0.43
	+nCPACPS	40	0.1576	218.7	2.840	0.41
		50	0.1385	218.7	2.495	0.32

[1] precision ± 0.0004.

TABLE II (Continued)

NO	*LC*	*T/°C*	*Δn(589 nm)*	*λ_0/nm*	*$G/10^{-6}$ nm^{-2}*	*$\sigma/10^{-3}$*
15	nPEP	20	0.1800	209.0	3.603	0.40
	+nCPEP	30	0.1741	208.7	3.494	0.39
		40	0.1670	208.5	3.360	0.35
		50	0.1580	208.3	3.187	0.34
		60	0.1466	208.1	2.964	0.39
		70	0.1335	207.9	2.705	0.45
16	nCPEPm	20	0.1292	202.2	2.788	0.49
		30	0.1273	201.9	2.755	0.49
17	nGCPEm	15	0.0370	187.4	0.947	0.14
18	nCPm	20	0.0747	152.2	3.009	0.24
	+PCNm	30	0.0701	152.0	2.832	0.25
	+nPCNm	40	0.0641	151.5	2.608	0.26
	+nOPANm	50	0.0550	148.9	2.322	0.32
	+nCANCPm					
19	nGCP	20	0.0990	178.1	2.836	0.27
	+nCEP	30	0.0885	182.2	2.412	0.29
20	nCEP	20	0.1188	175.7	3.505	0.43
		30	0.1157	174.1	3.484	0.40
		40	0.1103	176.9	3.207	0.37
		50	0.1037	176.8	3.017	0.38
		60	0.0943	177.0	2.738	0.37
21	nPZPOm	20	0.2631	254.5	3.305	1.43
		30	0.2503	254.0	3.158	1.34
		40	0.2352	253.1	2.994	1.16
22	nOPP(1)m	40	0.1440	229.5	2.320	1.22
		50	0.1467	231.2	2.323	1.07
		60	0.1431	232.1	2.245	1.01
		65	0.1378	235.2	2.093	0.97
		70	0.1004	235.2	1.525	0.71
23	nCE	20	0.0530	109.1	4.300	0.19
		30	0.0515	112.5	3.918	0.20
		40	0.0499	108.5	4.098	0.22
		50	0.0458	107.0	3.868	0.25
		60	0.0375	105.8	3.242	0.18
		70	0.0300	92.7	3.405	0.13
24	nPZZPOm	30	0.3620[2]	264.9	4.114	1.88
		40	0.3519[1]	264.6	4.012	1.97
25	nOPP	20	0.2450	255.8	3.038	1.64
		30	0.2330	255.6	2.894	1.54
		40	0.2198	255.5	2.733	1.39
		50	0.2029	255.4	2.525	1.21
26	nCPOm	20	0.0748	153.7	2.953	0.60
		30	0.0540	154.4	2.110	0.22

[2] precision ± 0.0014.

TABLE II (Continued)

NO	*LC*	*T/°C*	*Δn(589 nm)*	*λ_0/nm*	*$G/10^{-6}$ nm^{-2}*	*$\sigma/10^{-3}$*
27	nDP	20	0.1069	170.5	3.370	0.42
		30	0.0959	167.7	3.135	0.30
		40	0.0752	170.5	2.369	0.19
28	nCECm	20	0.0415	100.3	4.003	0.11
		30	0.0370	104.5	3.280	0.09

TABLE III Ordinary refractive indices of liquid crystal mixtures from refractometric and spectroscopic measurements. Fit parameters λ_0 and G_0 and standard deviations σ refer to Equation 8b

NO	*LC*	*T/C°*	*n_o(589 nm)*	*λ_0/nm*	*$G_0/10^{-5}$nm^{-2}*	*$\sigma/10^{-3}$*
1	nCP	20	1.4904	103.3	4.457	0.67
		30	1.4888	103.5	4.424	0.64
		40	1.4879	105.5	4.246	0.61
		50	1.4905	104.8	4.321	0.69
2	nCP	20	1.4974	108.1	4.117	0.85
		30	1.5003	110.5	3.955	0.63
3	nCEPOm	20	1.4808	99.8	4.692	0.43
		30	1.4779	99.1	4.725	0.62
		40	1.4759	99.0	4.720	0.55
		50	1.4739	98.9	4.704	0.46
4	nCEPOm	20	1.4801	96.2	5.045	0.76
		30	1.4772	99.7	4.666	1.10
		40	1.4747	98.2	4.787	0.50
		50	1.4723	98.4	4.746	0.50
5	nCPS	20	1.5217	123.2	3.288	0.78
		30	1.5225	124.7	3.210	0.79
6	nCPS	20	1.5215	125.8	3.147	0.99
		30	1.5227	126.8	3.099	1.12
7	nPP	20	1.5295	136.2	2.703	0.76
		30	1.5339	140.2	2.562	0.57
8	nPEP	20	1.5104	125.3	3.102	2.07
		30	1.5108	128.1	2.966	1.97
		40	1.5133	129.0	2.939	1.13
9	nCAPF	20	1.4862	90.8	5.763	0.50
	+nCPAPm	30	1.4840	93.4	5.405	0.47
		40	1.4820	91.8	5.579	0.50
10	nPACOm	20	1.4851	100.1	4.700	0.40
		30	1.4830	99.9	4.705	0.51
		40	1.4815	99.4	4.734	0.44
11	nPEPOm	20	1.5002	113.3	3.751	0.66
	+nOPEPOm	30	1.4990	113.2	3.749	0.95
		40	1.4983	114.6	3.652	0.84
		50	1.4982	114.4	3.664	0.98

TABLE III (Continued)

NO	*LC*	*T/C°*	n_o(589 nm)	λ_0/nm	$G_0/10^{-5}\,nm^{-2}$	$\sigma/10^{-3}$
12	nBEPF	20	1.4874	98.1	4.930	0.46
		30	1.4858	97.9	4.926	0.44
13	nCAPF	20	1.4923	106.0	4.239	0.71
	+nBAPPF	30	1.4903	105.4	4.272	0.63
14	nCPS	30	1.5250	123.4	3.298	0.67
	+nCPACPS	40	1.5248	129.9	2.960	1.40
		50	1.5262	124.0	3.271	0.69
15	nPEP	20	1.5065	118.3	3.472	0.64
	+nCPEP	30	1.5050	120.9	3.309	0.82
		40	1.5030	119.8	3.361	0.65
		50	1.5020	121.1	3.278	0.57
		60	1.5016	122.2	3.215	0.82
		70	1.5020	124.0	3.121	0.78
16	nCPEPm	20	1.5096	118.1	3.507	0.68
		30	1.5065	117.8	3.502	0.64
17	nGCPEm	15	1.5090	116.5	3.605	0.59
18	nCPm	20	1.4965	98.7	4.952	0.70
	+PCNm	30	1.4941	100.8	4.724	0.84
	+nPCNm	40	1.4918	99.2	4.852	0.70
	+nOPANm	50	1.4906	100.9	4.676	0.81
	+nCANCPm					
19	nGCP	20	1.4950	107.6	4.133	0.62
	+nCEP	30	1.4950	106.5	4.218	0.61
20	nCEP	20	1.4821	106.3	4.130	1.77
		30	1.4795	101.4	4.524	0.63
		40	1.4774	104.6	4.225	0.50
		50	1.4755	103.7	4.281	0.58
		60	1.4744	104.1	4.243	0.51
21	nPZPOm	20	1.5172	129.7	2.925	0.49
		30	1.5172	134.9	2.692	0.86
		40	1.5178	135.5	2.671	0.59
22	nOPP(1)m	40	1.4840	96.0	5.118	1.34
		50	1.4821	99.5	4.728	0.91
		60	1.4799	97.2	4.941	0.70
		65	1.4802	105.2	4.205	0.62
		70	1.4896	104.5	4.342	0.62
23	nCE	20	1.4560	80.4	6.920	0.61
		30	1.4525	81.1	6.748	0.44
		40	1.4496	80.0	6.896	0.45
		50	1.4462	78.4	7.125	0.44
		60	1.4430	79.5	6.877	0.45
		70	1.4400	79.2	6.889	0.31
24	nPZZPOm	30	1.5210[1]	145.3	2.317	0.70
		40	1.5213[2]	145.7	2.305	0.81

[1] precision ±0.001.

[2] precision ±0.0003.

TABLE III (Continued)

NO	*LC*	*T/C°*	$n_o(589\,nm)$	λ_0/nm	$G_0/10^{-5}\,nm^{-2}$	$\sigma/10^{-3}$
25	nOPP	20	1.5206	135.0	2.705	0.85
		30	1.5198	137.9	2.583	0.69
		40	1.5198	140.3	2.491	1.00
		50	1.5209	140.8	2.479	0.46
26	nCPOm	20	1.4934	105.1	4.322	0.46
		30	1.4950	107.4	4.151	0.94
27	nDP	20	1.4853	106.0	4.178	0.85
		30	1.4848	107.5	4.055	0.63
		40	1.4870	109.3	3.938	0.98
28	nCECm	20	1.4604	87.8	5.846	0.71
		30	1.4578	85.7	6.099	0.78

TABLE IV Extraordinary refractive index of liquid crystal mixtures from refractometric and spectroscopic measurements. Fit parameters λ_e and G_e and standard deviations σ refer to Equations 8b

NO	*LC*	*T/C°*	$n_e(589\,nm)$	λ_e/nm	$G/10^{-5}\,nm^{-2}$	$\sigma/10^{-3}$
1	nCP	20	1.6117	123.3	3.849	0.60
		30	1.6018	121.3	3.918	0.56
		40	1.5902	121.4	3.837	0.69
		50	1.5691	119.2	3.841	0.62
2	nCP	20	1.5977	125.7	3.612	0.90
		30	1.5763	125.5	3.494	0.63
3	nCEPOm	20	1.5622	112.7	4.267	0.58
		30	1.5555	111.5	4.309	0.55
		40	1.5484	111.1	4.289	0.43
		50	1.5401	108.7	4.416	0.60
4	nCEPOm	20	1.5678	112.5	4.321	0.88
		30	1.5612	115.4	4.054	1.37
		40	1.5544	114.2	4.089	1.38
		50	1.5468	111.4	4.245	1.35
5	nCPS	20	1.7156	160.5	2.571	0.88
		30	1.7008	158.9	2.575	0.72
6	nCPS	20	1.6792	156.7	2.569	0.90
		30	1.6631	154.6	2.584	0.88
7	nPP	20	1.7267	178.6	2.069	1.77
		30	1.7046	175.7	2.079	1.24
8	nPEP	20	1.6763	153.5	2.677	2.37
		30	1.6622	153.1	2.633	2.44
		40	1.6435	150.9	2.642	1.49
9	nCAPF +nCPAPm	20	1.5552	100.0	5.393	0.59
		30	1.5490	102.1	5.106	0.47
		40	1.5415	100.0	5.262	0.47

TABLE IV (Continued)

NO	*LC*	*T/C*	$n_e(589\,nm)$	λ_e/nm	$G/10^{-5}\,nm^{-2}$	$\sigma/10^{-3}$
10	nPACOm	20	1.5691	111.2	4.442	0.49
		30	1.5623	110.1	4.481	0.51
		40	1.5543	107.7	4.618	0.60
11	nPEPOm	20	1.6405[1]	140.0	3.084	0.64
	+nOPEPOm	30	1.6345[1]	138.9	3.106	0.85
		40	1.6295	139.0	3.077	0.80
		50	1.6171	136.9	3.116	0.93
12	nBEPF	20	1.5443	103.5	4.922	0.41
		30	1.5369	101.4	5.064	0.35
13	nCAPF	20	1.5759	122.0	3.703	0.66
	+nBAPPF	30	1.5689	120.3	3.767	0.58
14	nCPS	30	1.6951	153.2	2.763	0.66
	+nCPACPS	40	1.6824	154.5	2.664	1.36
		50	1.6647	148.3	2.833	0.67
15	nPEP	20	1.6865	149.8	2.863	0.74
	+nCPEP	30	1.6791	149.8	2.829	0.87
		40	1.6700	147.9	2.871	0.71
		50	1.6600	147.8	2.830	0.62
		60	1.6482	146.7	2.823	0.80
		70	1.6355	146.0	2.797	0.87
16	nCPEPm	20	1.6388	141.6	3.004	0.57
		30	1.6338	140.8	3.015	0.53
17	nGCPEm	15	1.5460	122.3	3.491	0.61
18	nCPm	20	1.5712	108.2	4.713	0.78
	+PCNm	30	1.5642	109.5	4.545	0.84
	+nPCNm	40	1.5559	107.9	4.612	0.74
	+nOPANm	50	1.5456	108.1	4.511	0.68
	+nCANCPm					
19	nGCP	20	1.5940	123.6	3.717	0.63
	+nCEP	30	1.5835	122.7	3.706	0.48
20	nCEP	20	1.6009	124.7	3.689	1.73
		30	1.5952	120.5	3.929	0.57
		40	1.5877	122.5	3.747	0.62
		50	1.5792	120.8	3.803	0.57
		60	1.5687	120.2	3.771	0.61
21	nPZPOm	20	1.7803	192.3	1.885	3.17
		30	1.7675	191.7	1.868	3.64
		40	1.7530	188.6	1.900	2.52
22	nOPP(1)m	40	1.6280	152.0	2.537	2.45
		50	1.6288	153.5	2.489	2.21
		60	1.6230	152.4	2.503	1.62
		65	1.6180	153.6	2.442	2.16
		70	1.5900	143.9	2.678	1.70

[1] precision ±0.0003.

TABLE IV (Continued)

NO	*LC*	*T/C°*	n_e*(589 nm)*	λ_e*/nm*	$G/10^{-5}\,nm^{-2}$	$\sigma/10^{-3}$
23	nCE	20	1.5090	84.9	6.909	0.59
		30	1.5040	85.9	6.684	0.41
		40	1.4995	83.7	6.980	0.48
		50	1.4920	82.5	7.080	0.41
		60	1.4805	82.4	6.938	0.41
		70	1.4700	80.1	7.193	0.32
24	nPZZPOm	30	1.8830[2]	212.8	1.696	4.58
		40	1.8732[1]	211.4	1.703	4.29
25	nOPP	20	1.7656	193.1	1.832	3.36
		30	1.7528	192.4	1.816	3.73
		40	1.7396	191.5	1.803	3.89
		50	1.7238	188.9	1.820	3.05
26	nCPOm	20	1.5682	115.6	4.087	0.72
		30	1.5490	114.2	4.050	0.88
27	nDP	20	1.5922	122.2	3.797	0.67
		30	1.5807	120.6	3.824	0.59
		40	1.5622	119.8	3.756	1.00
28	nCECm	20	1.5019	88.0	6.333	0.73
		30	1.4948	86.7	6.442	0.80

[1] precision ± 0.0003.
[2] precision ± 0.001.

The standard deviation σ between fit (Equation 8) and experimental data is given in the last column.

Some regularities are observed in the presented data. For example mixtures with even and odd numbers of carbon atoms in their alkyl chains possess rather different birefringence [15], lower for even members and higher for odd members, but their dispersion characteristic is similar. This is obvious if one compares the wavelength dependence of the birefringence normalized to 1 at one wavelength (say 589 nm). In doing so the factor G in Equation 8a vanishes and it is seen that the resonance wavelength determines dispersion.

In Figure 3 the normalized dispersion of some mixtures is plotted, showing the equality of dispersion for mixtures differing only in their alkyl chains. Birefringence dispersion of biphenyls with ester linking group (mixtures 8, 11, 15 and 16) seems to be remarkably insensitive to the terminal groups used while the clearing temperature raises drastically within this series.

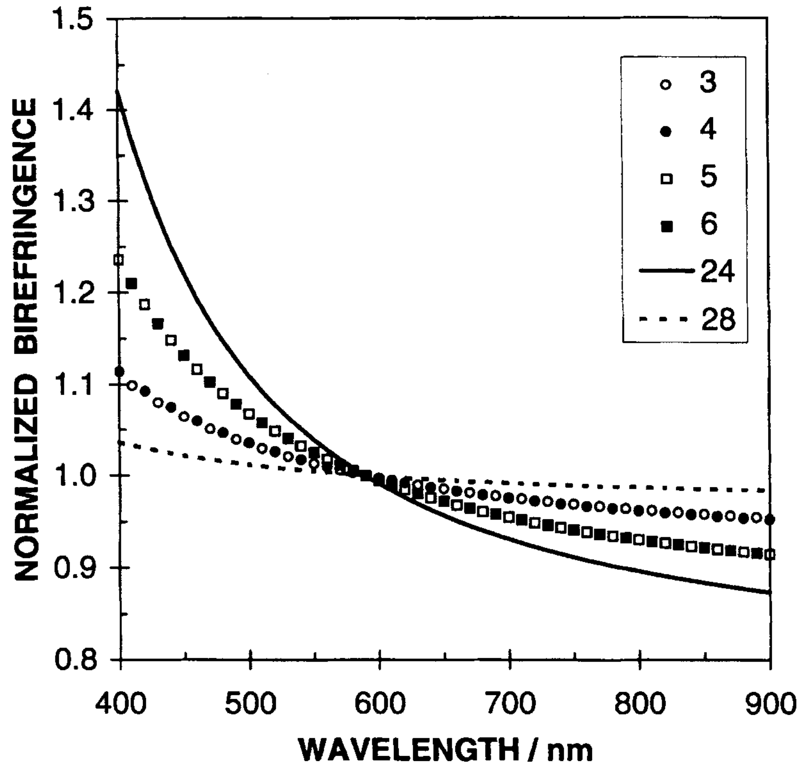

FIGURE 3 Comparison of birefringence dispersion for some LC's studied. Values are normalized to 1 at 589 nm and plotted for 20°C. Numbers identify the mixtures. Refer to Table I for numbers and compositions of mixtures.

CONCLUSION

The birefringence and refractive indices dispersion curves of 28 LC mixtures, most of them composed of homologous compounds and being nematic at room temperature, have been measured for various temperatures in the wavelength region 400 to 900 nm. Homologous with odd and even numbers of carbon atoms in the alkyl chains are found to have similar dispersion of birefringence, although the absolute value is quite different. The set of LC mixtures presented in this work covers a considerable range of absolute values and dispersions in both birefringence and refractive indices. It can therefore serve as a data base for selecting LC mixtures and for designing new mixtures.

Acknowledgement

This work was supported by the European Community, grant CIPA-CT94-0157.

APPENDIX: PHASE SHIFT DUE TO ITO AND POLYIMIDE FILMS

The ordinary refractive index of the LC's studied is in the range 1.45–1.55. For polyimide we got the information $n_p \approx 1.55$ from the producer of the LC cells. Taking dispersion into account the values $n_p \approx 1.58$, 1.55, 1.54 for wavelengths 400 nm, 589 nm, 900 nm are realistic. The refractive index of glass is $n_g \approx 1.53$, 1.52 and 1.51 at 400 nm, 589 nm and 900 nm. In contrast from the producers information and our own measurements of the Brewster angle for a disassembled cell the refractive index of ITO is $n_I \approx 2.2$, 1.8 and 1.7 for wavelengths 400 nm, 589 nm and 900 nm. Thus we may neglect reflections at the LC to polyimide surface (which are in addition suppressed by the nonuniform surface quality due to the rubbing process) and calculate with the model depicted in Figure A1. We also neglect higher order terms since reflection coefficients are sufficiently small.

The phase retardation δ_x for the ordinary wave due to one passage of the LC layer and the two polyimide films is:

$$\delta_x = \delta_o + 2\delta_p = 2\pi \frac{n_o d_{\mathrm{LC}} + 2n_p d_p}{\lambda} \tag{A1}$$

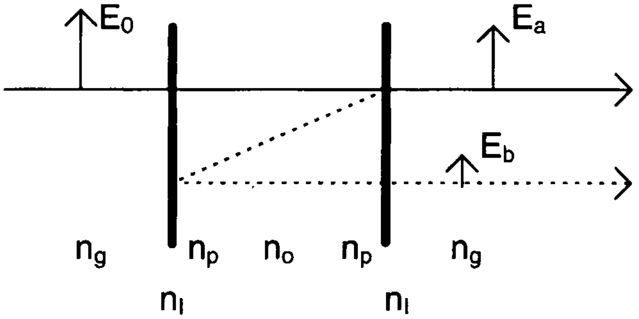

FIGURE A1 Model for calculation of the phase change due to reflection at ITO films. E_0 is the incoming electric field, E_a the directly transmitted one and E_b the portion reflected at the ITO films. The refractive index n_I of ITO is considerably higher than that of glass (n_g), polyimide (n_p) and the LC (n_o).

We denote with φ_r and φ_t the phase changes caused by reflection at or transmission of one ITO film and with r and t the reflection and transmission coefficients for the electrical field. The measured field and intensity are ($t^2 = 1 - r^2 = 1 - R$ with R = intensity reflection coefficient if absorption is neglected):

$$\begin{aligned} E_{\text{out}} &= E_a + E_b \\ &= E_0 t^2 \exp(2i\varphi_t)\exp(-i\delta_x)[1 + r^2 \exp(2i\varphi_r)\exp(-2i\delta_x)] \\ I_{\text{out}} &= E_{\text{out}} \cdot E^*_{\text{out}} \\ &= I_0(1-R)^2[1 + R^2 + 4R\cos(2\delta_x - 2\varphi_r)] \end{aligned} \tag{A2}$$

Transmission maxima are found for wavelengths λ_k where the term $(2\delta_x - 2\varphi_r)$ equals a multiple of 2π. Combining this condition with Equation A1 leads to Equation 7 used for refractive index determination.

The additional phase shift φ_r due to reflection at ITO can be evaluated from the matrix theory for thin film systems [16]. For normal incidence the field in the incident medium (here polyimide) is described by the electric and magnetic vectors E and H with:

$$\begin{pmatrix} E \\ H \end{pmatrix} = \begin{pmatrix} \cos\delta_I & i/n_I \sin\delta_I \\ in_I \sin\delta_I & \cos\delta_I \end{pmatrix} \begin{pmatrix} 1 \\ n_g \end{pmatrix} \tag{A3}$$

$\delta_I = 2\pi n_I d_I/\lambda$ is the phase change due to one passage of the ITO film. The reflection coefficient r and the phase shift on reflection φ_r are:

$$\begin{aligned} r &= \frac{r_1}{r_2} = \frac{(n_p E - H)}{(n_p E + H)} \\ \varphi_r &= \arg r = \tan^{-1}\left(\frac{\operatorname{Im} r_1}{\operatorname{Re} r_1}\right) - \tan^{-1}\left(\frac{\operatorname{Im} r_2}{\operatorname{Re} r_2}\right) \\ &= \tan^{-1}\left(\frac{n_g n_p - n_I^2}{n_I(n_p - n_g)}\tan\delta_I\right) - \tan^{-1}\left(\frac{n_g n_p + n_I^2}{n_I(n_p + n_g)}\tan\delta_I\right) \end{aligned} \tag{A4}$$

The fraction in the first term has a high negative value ($n_p > n_g$, $n_p \approx n_g$ and $n_p \ll n_I$) while the fraction in the second term is close to 1. Thus

Equation A4 can be simplified:

$$\varphi_r \approx -\frac{\pi}{2} - \delta_I \tag{A5}$$

For very thin ITO films ($\delta_I \ll 1$) the two reflections cause an interchange of interference maxima and minima. It is also seen that the refractive indices of polyimide and glass have no significant impact on the correction term as long as they are small compared to the refractive index of ITO.

With the limiting values for the thicknesses of ITO and polyimide films stated by the LC cell producer we find possible errors in refractive index determination of up to ± 0.008. However the wavelength dependence of these errors is small so that after calibration with the refractometric data at 589 nm the uncertainty reduces to less than ± 0.002.

Depending on deposition conditions the refractive index of ITO may differ as much as ± 0.1 from the values stated above. The resulting error in refractive index determination is calculated to be less than ± 0.003 as long as the refractive index of ITO is larger than 1.65. Otherwise the intensity reflection coefficient becomes lower than 0.2% and it is no longer possible to find reliable positions of interference maxima due to the experimental scattering of the data.

References

[1] T. Oh-ide, M. Higa and K. Fujimura, *Proc. of Asia Display '95*, October 1995, **Hamamatsu**, p. 169.
[2] I. Fukuda, M. Kitamura and Y. Kotani, *Proc. of Asia Display '95*, October 1995, **Hamamatsu**, p. 881.
[3] M. F. Flynn and P. J. Bos, *SID '95 Digest*, May 1995, **Orlando**, p. 801.
[4] J. I. Hirakata, H. Abe, I. Hiyama and K. Kondo, *SID'95 Digest*, May 1995, **Orlando**, p. 563.
[5] V. Konovalov, A. Muravski, S. Yakovenko, A. Smirnov and A. Usenok, *SID'94 Digest*, June 1994, **San Jose**, p. 615.
[6] D. J. Boer, *SID'95 Digest*, May 1995, **Orlando**, p. 165.
[7] S. T. Wu, U. Efron and La Verne, D. Hess, *Appl. Opt.*, **23**, 3911 (1984).
[8] D. Kinzer, *Mol. Cryst Liq. Cryst. Lett.*, **5**, 147 (1985).
[9] S. T. Wu and K. C. Lim, *Appl. Opt.*, **26**, 1722 (1987).
[10] P. Kohns, J. Schirmer, A. A. Muravski, S. Y. Yakovenko, V. Bezborodow and R. D. Dabrowski, *Liq. Cryst.*, **21**, 841–846 (1996).
[11] V. Bezborodow, G. Sosnovskij, R. D. Dabrowski, J. Dziaduszek, J. Schirmer and P. Kohns, *Liq. Cryst.*, **21**, 237 (1996).
[12] T. Szczucinski, R. Dabrowski, J. Parka and J. Kedzierski, SPIE *Proc. European Conference on Liquid Crystals*, Zallopane, Poland 1997 (in press).
[13] V. Vill, in *Landolt-Börnstein, Liquid Crystals* (Springer Verlag, **Berlin**, 1992), ed. by J. Thiem, Series IV/7a and IV/7b.

[14] I. C. Khoo and S. T. Wu, *Optics and Nonlinear Optics of Liquid Crystals* (World Scientific, **Singapore** 1993), Chap 1.
[15] G. Pelzl and A. Hauser, *Phase Transitions*, **37**, 33 (1991).
[16] J. A. Dobrowolski, in *Handbook of Optics*, (McGraw-Hill, **New York**, 1995) 2nd ed., ed. by M. Bass, E. W. Van Stryland, D. R. Williams, W. L. Wolfe, Vol. 1, Chap 42.